BUKU PETUNJUK PRAKTIKUM

OPTIK

JURUSAN FISIKA

FAKULTAS SAINS DAN TEKNOLOGI

UNIVERSITAS ISLAM NEGERI MAULANA MALIK IBRAHIM

MALANG

2022

JUDUL PERCOBAAN

No.	JUDUL PERCOBAAN
1	MICHELSON INTERFEROMETER
2	MAGNETOSTRICTION WITH THE MICHELSON INTERFEROMETER
3	POLARISATION THROUGH λ/4 PLATES
4	DIFFRACTION INTENSITY OF MULTIPLE SLITS AND GRIDS

Michelson interferometer

LEP 2.2.05 -00

Related topics

Interference, wavelength, refractive index, velocity of light, phase, virtual light source.

Principle

In the Michelson arrangement interference will occur by the use of 2 mirrors. The wavelength is determined by displacing one mirror using the micrometer screw.

Equipment

Michelson interferometer	08557.00	1
Laser, He-Ne 1.0 mW, 220 V AC	08181.93	1
Swinging arm	08256.00	1
Lens, mounted, f = +20 mm	08018.01	1
Lens holder	08012.00	1
Slide mount f. opt. pr.-bench, h = 30 mm	08286.01	3
Optical profile bench l = 60 cm	08283.00	1
Base f. opt. profile-bench, adjust.	08284.00	2
Screen, metal, 300×300 mm	08062.00	1
Barrel base -PASS-	02006.55	1

Tasks

Determination of the wavelength of the light of the used laser.

Set-up and procedure

The experimental set up is as shown in Fig. 1. In order to obtain the largest possible number of interference fringes, the two mirrors of the interferometer are first of all adjusted; to do this, the lens is first of all removed. The laser beam strikes the half-silvered mirror at an angle of 45° splitting the beam. The resulting two beams are reflected by the mirror and impinge on the screen. By means of the two adjusting screws fitted to one of the mirrors, both points of light are made to coincide. If the lens is placed in the light beam, the points of light are enlarged and the interference patterns are observed on the screen (bands, circles). By careful readjustment, an interference image of concentric circles will be obtained.

To measure the wavelength, the micrometer screw is turned to any initial position at which the centre of the circles is dark. The micrometer screws is now further turned in the same direction and the light-dark periods thus produced are counted. The distance travelled by the mirror must be read off on the micrometer screw and divided by ten (lever reduction 1:10). Should the central point of the circles move outside the light spot area a readjustment has to be performed.

Caution: Never look directly into a non attenuated laser beam

Fig. 1: Experimental set-up for measuring wavelengths with the Michelson interferometer.

LEP 2.2.05 -00	Michelson interferometer

Fig. 2: Michelson interferometer set up.

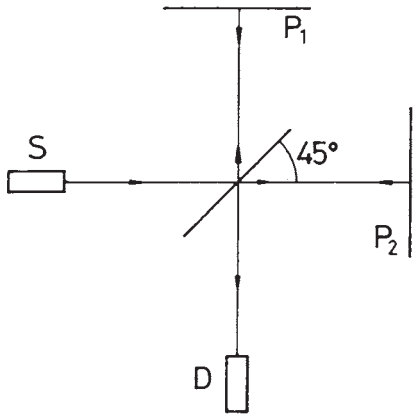

Fig. 3: Formation of circles on interference.

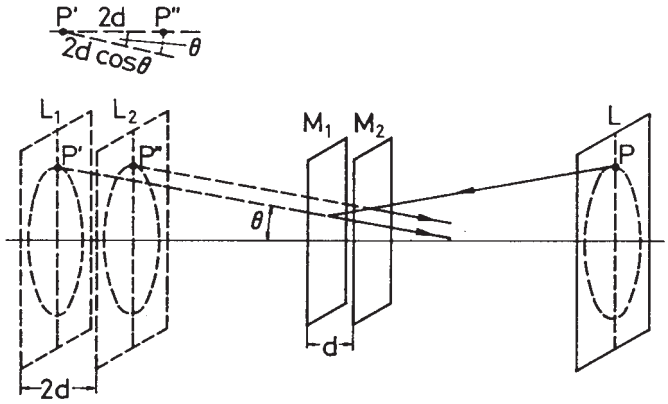

Theory and evaluation

If 2 waves of the same frequency ω but of different amplitude and different phase impinge on one point they are superimposed, or interfere, so that:

$$y = a_1 \sin(\omega t - \alpha_1) + a_2 \sin(\omega t - \alpha_2).$$

The resulting wave can be described as

$$y = A \sin(\omega t - \alpha)$$

with the amplitude

$$A^2 = a_1^2 + a_2^2 + 2a_1 a_2 \cos\delta \qquad (1)$$

and the phase difference

$$\delta = \alpha_1 - \alpha_2.$$

In a Michelson interferometer, light is split up into two beams by a half-silvered glass plate (amplitude splitting), reflected by two mirrors, and passed again through the glass plate to produce interference phenomena behind it.

A lens is inserted between the light beam and the glass plate so that the light source lies at the focal point, since only enlarged light spots can exhibit interference rings.

If the actual mirror $\mathbf{M_1}$ is replaced by its virtual image $\mathbf{M_1'} = \mathbf{M_2}$ which is formed by reflection at the glass plate, a point **P** of the real light source is formed as the points **P'** and **P"** of the virtual light sources $\mathbf{L_1}$ and $\mathbf{L_2}$.

Based on the different light paths, the phase difference, using the symbols of Fig. 3, is:

$$\delta = \frac{2\pi}{\lambda} 2d \cos\theta \qquad (2)$$

where λ is the wavelength of the light used in the experiment.

The intensity distribution for $a_1 = a_2 = a$ according to (1) is:

$$I \sim A^2 = 4a^2 \cos^2 \frac{\delta}{2} \qquad (3)$$

Maxima thus occur if δ is a multiple of 2π, i.e. from equation (2), if

$$2d \cos\theta = m\lambda;\ m = 1, 2, \ldots \qquad (4)$$

i.e. circles are produced for a fixed value of m and d since θ remains constant (see Fig. 3).

If the position of the movable mirror $\mathbf{M_1}$ is changed so that d for example decreases then, according to equation (4), the diameter of the ring will also decrease since m is fixed for this ring. A ring thus dissapears each time d is reduced by $\lambda/2$. The ring pattern disappears if $d = 0$.

If $\mathbf{M_1}$ and $\mathbf{M_2}$ are not parallel, curved bands are obtained which are converted to straight bands when $d = 0$.

To measure the wavelength of the light, 500 ring changes were counted. A 158 μm displacement of the mirrow was measured. From this, the wavelength was obtained as:

$$\lambda = 632 \text{ nm}.$$

Magnetostriction with the Michelson interferometer

LEP 4.3.08 -00

Related terms
Interference, wavelength, diffraction index, speed of light, phase, virtual light source, ferromagnetic material, Weiss molecular magnetic fields, spin-orbit coupling.

Principle
With the aid of two mirrors in a Michelson arrangement, light is brought to interference. Due to the magnetostrictive effect, one of the mirrors is shifted by variation in the magnetic field applied to a sample, and the change in the interference pattern is observed.

Equipment

Base plate with rubber feet	08700.00	1
HeNe Laser, 1 mW*	08180.93	1
Adjusting support, 35 x 35 mm	08711.00	3
Surface mirror, 30 x 30 mm	08711.01	4
Magnetic base	08710.00	7
Plate holder	08719.00	1
Beam splitter, 50:50	08741.00	1
Lens with mount, f = +20 mm	08018.01	1
Lens holder for base plate	08723.00	1
Screen, white, 150 x 150 mm	09826.00	1
Coil, N = 1200, 4 Ω, Faraday Modulator	08733.00	1
Metal rods for magnetostriction	08733.01	1
Power supply, universal	13500.93	1
Digital multimeter	07134.00	1
Battery, 9 V, 6 F22	07496.10	1
Connecting cord, l = 500 mm, blue	07361.04	1

*alternative:

HeNe Laser, 5 mW	08701.00	1
Power supply and switch for 5 mW Laser	08702.93	1

Tasks
- Construction of a Michelson interferometer using separate optical components.
- Testing various ferromagnetic materials (iron and nickel) as well as a non-ferromagnetic material (copper) with regard to their magnetostrictive properties.

Set-up and procedure
In the following, the pairs of numbers in brackets refer to the co-ordinates on the optical base plate in accordance with Fig. 1. These co-ordinates are only intended to be a rough guideline for initial adjustment.
- Perform the experimental set-up according to Fig. 1 and 1a. The recommended set-up height (beam path height) is 130 mm.
- The lens **L** [1,7] must not be in position when making the initial adjustments.
- When adjusting the beam path with the adjustable mirrors $\mathbf{M_1}$ [1,8] and $\mathbf{M_2}$ [1,4], the beam is set along the 4th y co-ordinate of the base plate.
- Place mirror $\mathbf{M_3}$ onto the appropriate end of a sample (nickel or iron rod) – initially without the beam splitter **BS** [6,4] – and screw it into place.

Fig. 1. Experimental set-up

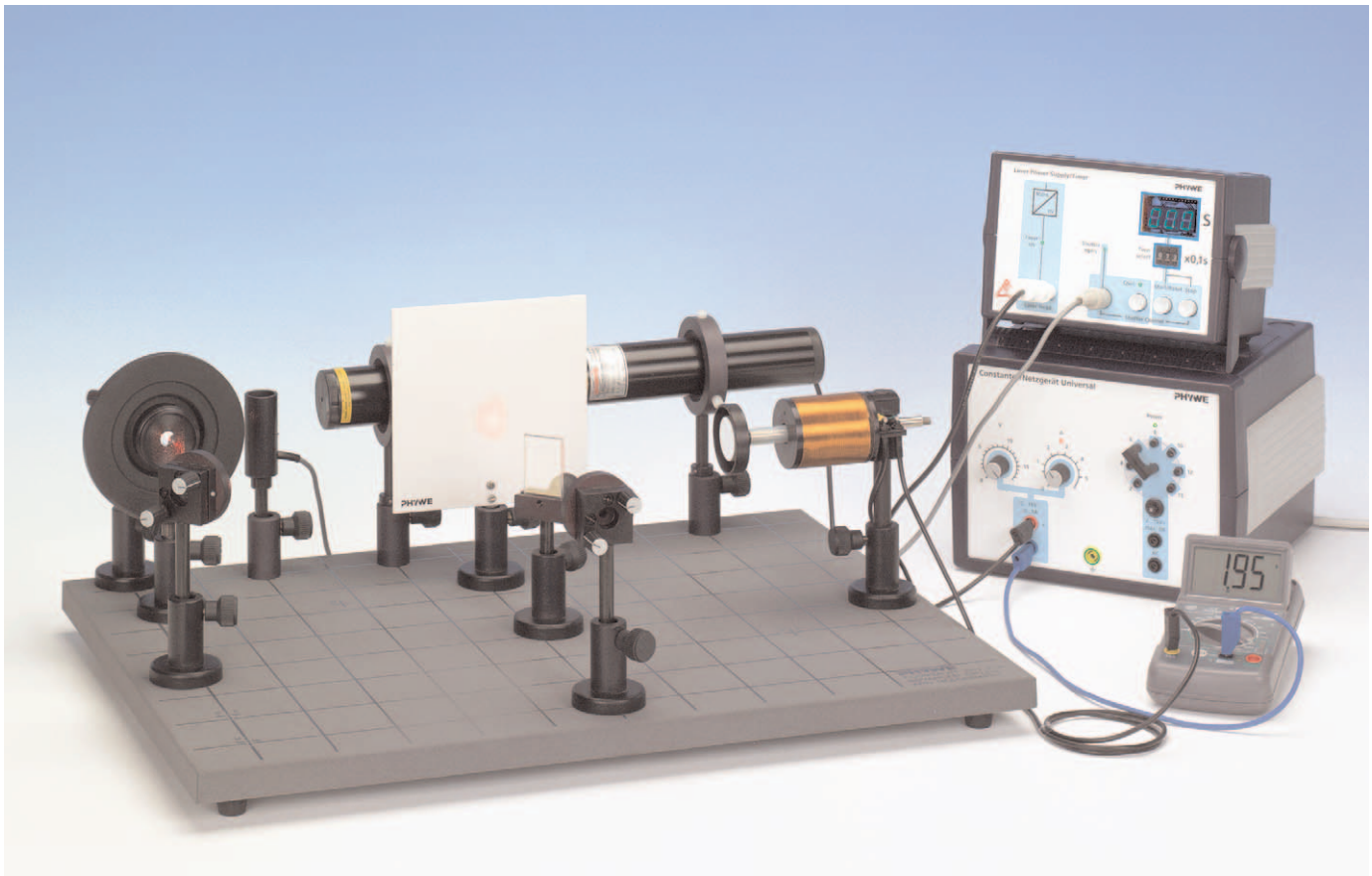

LEP 4.3.08 -00

Magnetostriction with the Michelson interferometer

– Now, insert the sample into the coil in such a manner that approximately the same length extends beyond the coil on both ends so that a uniform magnetisation can be assumed for the measurement. Fix the sample in position with the laterally attached knurled screw.
– Next, insert the coil **C**'s shaft into a magnetic base and place it at position [11,4] such that the mirror's plane is perpendicular to the propagation direction of the laser's beam (see Fig. 1a).
– Adjust the beam in a manner such that the beam reflected by mirror $\mathbf{M_3}$ once again coincides with its point of origin on mirror $\mathbf{M_2}$. This can be achieved by coarse shifting of the complete unit of coil with magnetic base or by turning the sample rod with mirror $\mathbf{M_3}$ in the coil and by meticulously aligning mirror $\mathbf{M_2}$ [1,4] with the aid of its fine adjustment mechanism.
– Next, position the beam splitter **BS** [6, 4] in such a manner that one partial beam still reaches mirror $\mathbf{M_3}$ without hindrance and the other partial beam strikes mirror $\mathbf{M_4}$ [6, 1]. Die metallized side of **BS** is facing mirror $\mathbf{M_4}$.
– Two luminous spots now appear on the screen **SC** [6, 6]. Make them coincide by adjusting the mirror $\mathbf{M_4}$ until a slight flickering of the luminous spot can be seen.
– After positioning lens **L** [1,7], an illuminated area with interference patterns appears on the screen. To obtain concentric circles, meticulously readjust mirror $\mathbf{M_4}$ using the adjustment screws.
– Subsequent to the connection of the coil to the power supply (connect the multimeter in series between the coil and the power supply to measure the current, measuring range 10 AC!), set the DC-voltage to maximum and DC-current to minimum value. Then slowly readjust the current. For the measurements the resulting currents lie between 0.5 and, maximally, 5 A. Count the changes from maximum to maximum (or minimum to minimum) in the interference pattern. In addition, pay attention to the direction in which the circular interference fringes move (sources or sinks!).
Repeat this procedure using different samples and different current strengths I between 0.5 and 5.0 A (I > 3 A only for a short time!).
– Notes:
The materials require a certain amount of premagnetisation; therefore, the current should be run up and down several times for each individual determination before performing the intensity change measurement.
The blank trial with a copper rod as sample should serve to demonstrate that the longitudinal deformation effect is due to magnetostriction and not to other causes.

Theory and evaluation

If two waves having the same frequency ω but different amplitudes and different phases are coincident at one location, they superimpose to

$$Y = a_1 \cdot \sin(\omega t - \alpha_1) + a_2 \cdot \sin(\omega t - \alpha_2).$$

Fig. 1a. Experimental set-up of the Michelson interferometer for the measurement of magnetostriction of different ferromagnetic materials (*only necessary with the 5-mW laser)

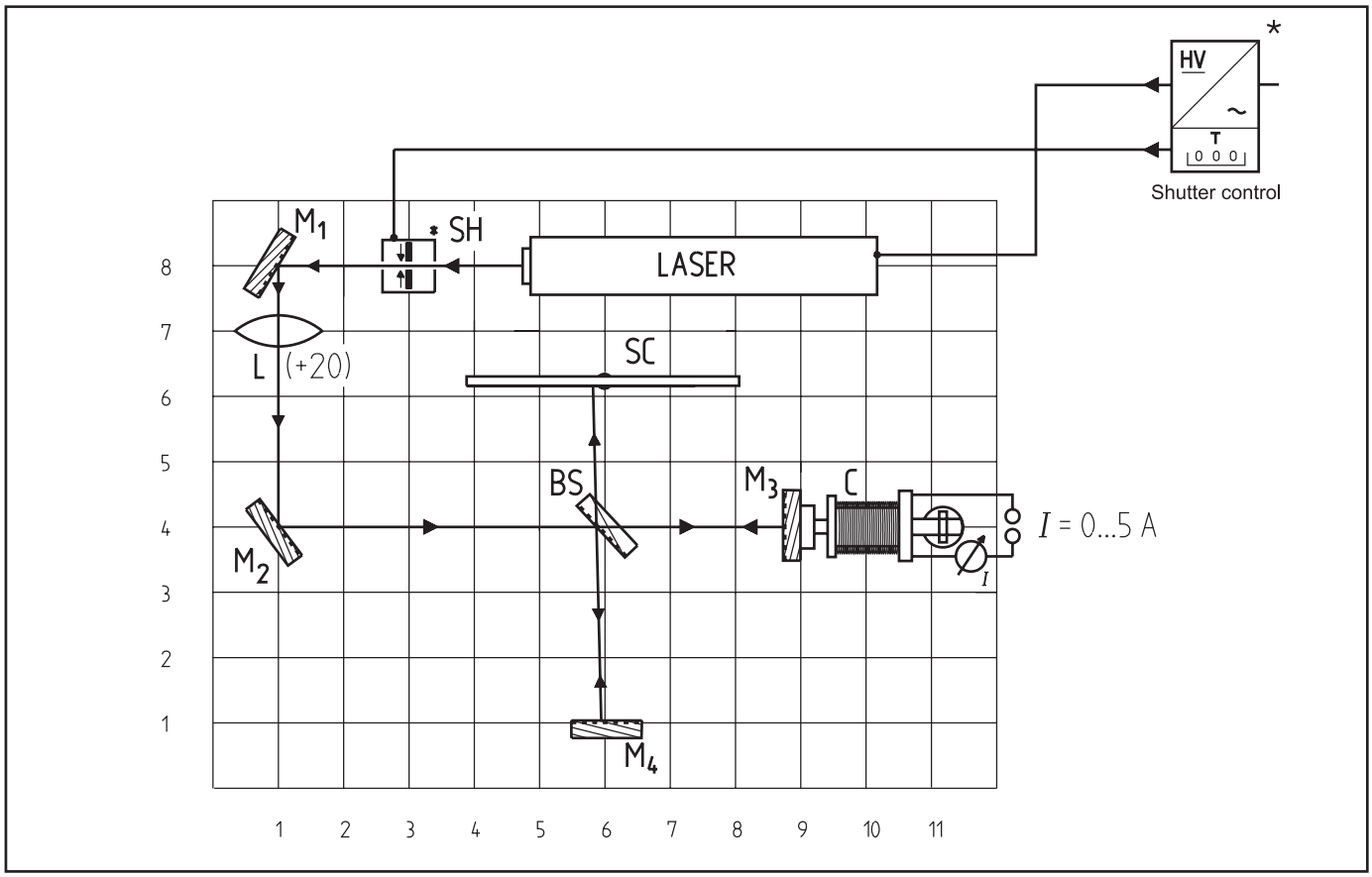

The resulting wave can be described by the following:

$$Y = A \cdot \sin(\omega t - \alpha)$$

with the amplitude

$$A^2 = a_1^2 + a_2^2 + 2\, a_1 a_2 \cdot \cos\delta \qquad (1)$$

and the phase difference

$$\delta = \alpha_1 - \alpha_2 .$$

In a Michelson interferometer, the light beam is split by a half-silvered glass plate into two partial beams (amplitude splitting), reflected by two mirrors, and again brought to interference behind the glass plate (Fig. 2). Since only large luminous spots can exhibit circular interference fringes, the light beam is expanded between the laser and the glass plate by a lens **L**.
If one replaces the real mirror $\mathbf{M_4}$ with its virtual image $\mathbf{M_4'}$,which is formed by reflection by the glass plate, a point **P** of the real light source appears as the points **P'** and **P"** of the virtual light sources $\mathbf{L_1}$ and $\mathbf{L_2}$.
As a consequence of the different light paths traversed, and using the designations in Fig. 3, the phase difference is given by:

$$\delta = \frac{2\pi}{\lambda} \cdot 2 \cdot d \cdot \cos\Theta \qquad (2)$$

λ is the wavelength of the laser light used.

According to (1), the intensity distribution for $a_1 = a_2 = a$ is:

$$I \sim A^2 = 4 \cdot a^2 \cdot \cos^2 \frac{\delta}{2} \qquad (3)$$

Maxima thus occur when δ is equal to a multiple of 2π, hence with (2)

$$2 \cdot d \cdot \cos\Theta = m \cdot \lambda \,;\, m = 1, 2, \ldots \qquad (4)$$

i.e. there are circular fringes for selected, fixed values of m, and d, since Θ remains constant (see Fig.3).
If one alters the position of the movable mirror $\mathbf{M_3}$ (cf. Fig.1) such that d, e.g., decreases, according to (4), the circular fringe diameter would also diminish since m is indeed defined for this ring. Thus, a ring disappears each time d is reduced by $\lambda/2$. For $d = 0$ the circular fringe pattern disappears. If the surfaces of mirrors $\mathbf{M_4}$ and $\mathbf{M_3}$ are not parallel in the sense of Fig. 3, one obtains curved fringes, which gradually change into straight fringes at $d = 0$.

Fig. 3. Formation of circular interference fringes

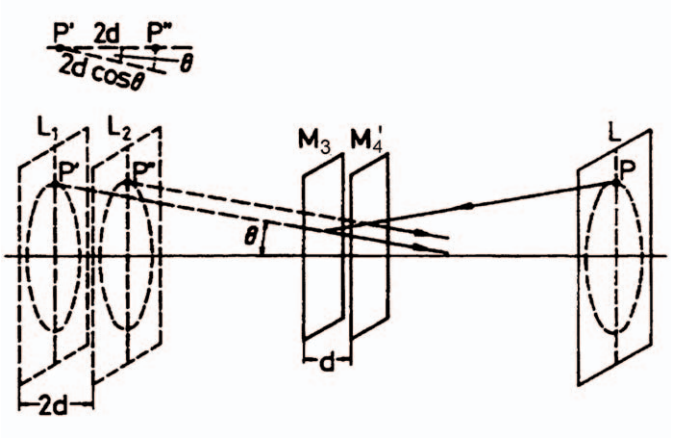

Fig. 2. Michelson arrangement for Interference. **S** represents the light source; **SC** the detector (or the position of the screen)

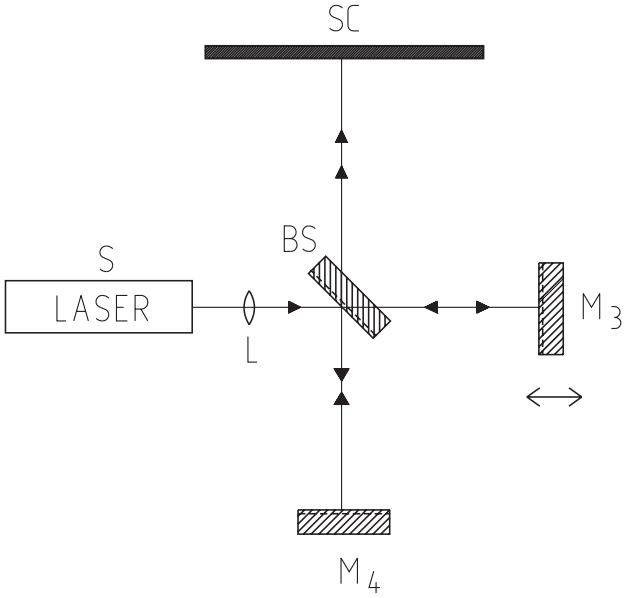

Fig.4: Magnetostriction of different ferromagnetic materials with their relative change in length $\Delta l / l$ plotted against applied magnetic field strength H_m

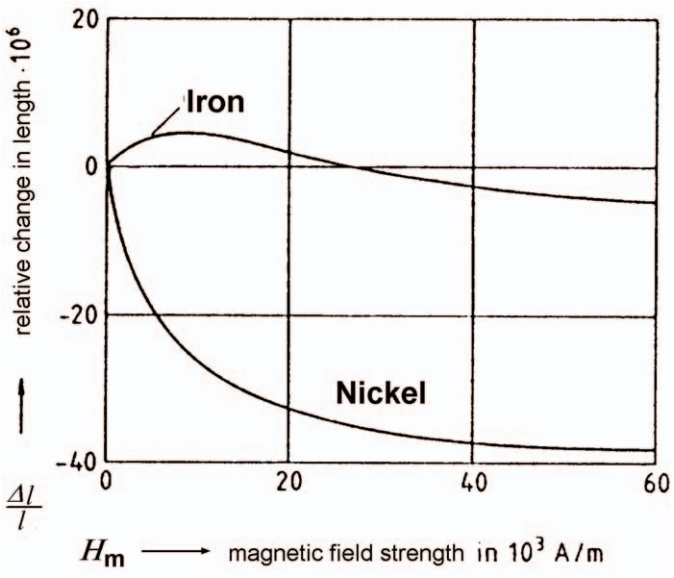

LEP 4.3.08 -00

Magnetostriction with the Michelson interferometer

On magnetostriction:
Ferromagnetic substances undergo so-called magnetic distortions, i.e. they exhibit a lengthening or shortening parallel to the direction of magnetisation. Such changes are termed positive or negative magnetostriction.
The distortions are on the order of $\Delta l/l \sim 10^{-8}$ to 10^{-4} in size. As is the case in crystal anisotropy, the magnetostriction is also ascribable to the spin-orbit mutual potential energy, as this is a function of the direction of magnetisation and the interatomic distances.
Due to magnetostriction, which corresponds to a spontaneous distortion of the lattice, a ferromagnet can reduce its total – anisotropic and elastic – energy.
Inversely, in cases of elastic tension the direction of spontaneous magnetisation is influenced. According to the principle of the least constraint, this means the following:
In cases of positive magnetostriction (in the case of iron (Fe)), under tensile stress the magnetisation is oriented parallel to the stress; in cases of compressive stress the magnetisation orients itself perpendicular to the pressure axis. In nickel (Ni) the situation is exactly reversed.
A true metal (ferromagnetic material) consists of small uniform microcrystals in dense packing, whose crystallographic axes are however irregularly distributed in all spatial directions.
The individual crystallites are additionally subdivided in Weiss molecular magnetic fields consisting of many molecules which form the elementary dipoles (*).
If the material has not been magnetised, all six (in nickel all eight) of the magnetic moment directions possible within a crystallite are present with equal frequency and consequently neutralise one another externally as a result of this irregular distribution. The magnetisation of the Weiss molecular magnetic fields is a function of temperature and occurs spontaneously below the Curie temperature .
However, as a consequence of the application of an external magnetic field this non-uniform distribution of the directions of magnetisation can be altered by the transition of a large number of Weiss molecular magnetic fields in the preferred light magnetisation directions, which have the smallest angle to the direction of the external magnetic field.

** On magnetic crystal anisotropy:*
In monocrystals one observes a marked anisotropy of the magnetisation curve. This is due to the so-called magnetic crystal energy. The source of this anisotropic energy in the transition metals (Fe, Ni and Co) is in their spin-orbit coupling energy, which is based on the relativistic interaction between spin and orbital movement.
In a rotation (directional alteration) of the spin, which is coupled by the mutual exchange energy, the orbital moments experience a torsional moment such that they also experience rotation. In an anisotropic electron distribution (d electrons) this effects a change in the overlapping of the electron clouds of adjacent atoms and hence an alteration of the total crystal energy.
One thus differentiates between the longitudinal magnetostriction, a length change parallel to the field direction and a transverse magnetostriction of the length alteration perpendicular to the external field direction.
The relative length change $\lambda = \Delta l/l$ generally increases with increasing magnetisation and reaches a saturation value λ_s at $M = M_s$ (M_s : saturation magnetisation)
The relative volume change $\Delta V/V$(i.e., volume magnetostriction) is usually considerably smaller, since longitudinal and transverse magnetostriction nearly always have opposite signs and compensate each other to a large extent.

In this experiment only the longitudinal magnetostriction is considered (see Fig. 4). One must take into consideration that the magnetostriction is a function of temperature and that premagnetisation is necessary. Additionally, the magnetostriction in alloys is also dependent on the composition of the metals and the appropriate pre-treatment (see Fig. 5).

Thermodynamic description of magnetostriction:
Magnetostriction can be described quantitatively and thermodynamically using:

S: elastic tension
s: elastic deformation (i.e.: $\Delta l/l$)
B: magnetic induction
H: Magnetic field strength
μ: magnetic permeability with

$$\frac{1}{\mu} = \frac{\partial H}{\partial B}$$

E: Elasticity module with

$$E = \frac{\partial S}{\partial s}$$

As a result of thermodynamic relationships, it can be shown that the direct and reciprocal magnetostriction effects are mutually linked via

$$\frac{\partial S}{\partial B} = \frac{1}{4\pi} \cdot \frac{\partial H}{\partial s} \qquad (5).$$

Fig. 5. Magnetostriction of different ferromagnetic alloys with their relative change in length $\Delta l/l$ plotted against applied field strength H_m

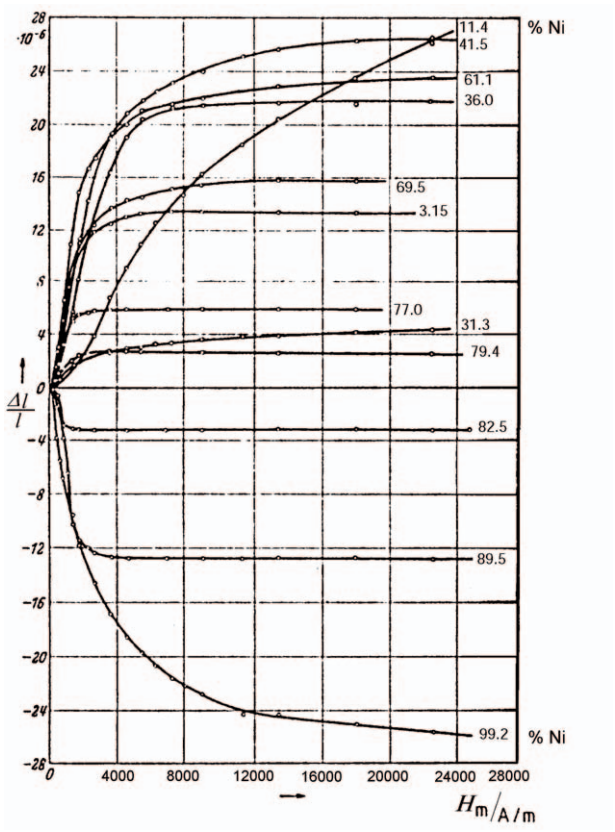

Magnetostriction with the Michelson interferometer

LEP 4.3.08 -00

For a free rod (unloaded and not clamped in position), the following is true:

$$s = -\gamma \cdot \frac{B}{E} \tag{6}$$

with the substance-specific quantity

$$\gamma = \frac{\partial S}{\partial B}.$$

In other words, the relative longitudinal change is given by

$$s = -\gamma \cdot \mu \cdot \frac{H}{E} \tag{7}$$

In this context, γ cannot be a constant as otherwise a linear increase in the relative length with the magnetic field strength would result. This is however not the case, since a saturation value is reached as of a specific field strength.

On the evaluation of the measuring results:
The magnetic field strength of a cylindrical coil is given by:

$$H_m = \frac{N \cdot I}{\sqrt{4 \cdot r^2 + l_s^2}} \tag{8}$$

where
H_m: magn. field strength at the centre of the coil in $A \cdot m^{-1}$
r: Radius of a winding (here: 0.024 m)
l_s: Length of the coil (here: 0.06 m)
N: Number of windings (here: 1200)

On condition that the field is homogenous, the field strength is by the following for $l >> r$:

$$H = \frac{N \cdot I}{l} \tag{9}$$

For this measurement we assume, as a first approximation, that the magnetic field strength H_m acts on the entire length of the rod (l = 0.15 m).
The alteration in length Δl is obtained from the number of circular fringe changes n; in the process the separation per circular fringe change alters by $\lambda/2$ (λ = 632 nm):

$$\Delta l = n \cdot \lambda/2. \tag{10}$$

In Tables (1) and (2) the results of the measurements on nickel and iron are summarised. In the measurements, the direction of magnetostriction also became apparent:
In iron the radii of the interference rings increased with increasing magnetic field strength (sources!); thus, the rod must have become larger (see Fig. 6 and Table 1).

Table 1

I/A	H/A/m (see (9))	Ring-changes/n	Δl/m (see (10))	$\Delta l/l$ with l =0.15 m
0.83	16600	≈ 1 1/4	$0.395 \cdot 10^{-6}$	$2.63 \cdot 10^{-6}$
1.27	25400	≈ 1 3/4	$0.554 \cdot 10^{-6}$	$3.691 \cdot 10^{-6}$
1.6	32000	≈ 1 1/2	$0.475 \cdot 10^{-6}$	$3.164 \cdot 10^{-6}$
1.87	37400	≈ 1 1/4	$0.395 \cdot 10^{-6}$	$2.630 \cdot 10^{-6}$

Fig. 6. Measuring results of the magnetostriction of iron (steel) with the relative change in length $\Delta l/l$ plotted against applied field strength H

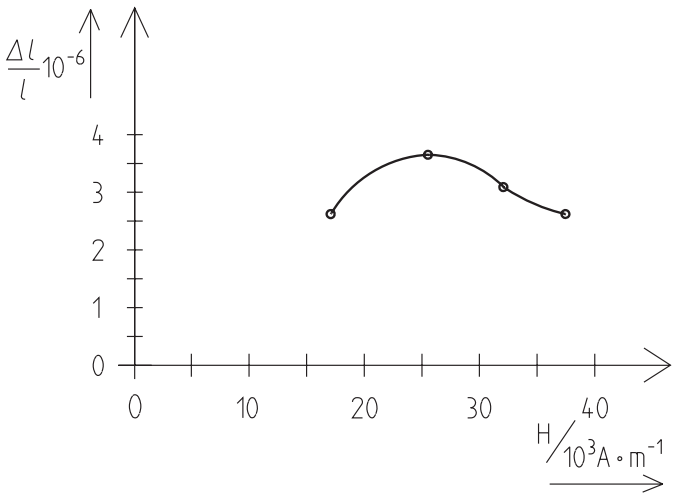

Fig. 7. Measuring results of the magnetostriction of nickel with the relative change in length $\Delta l/l$ plotted against applied field strength H

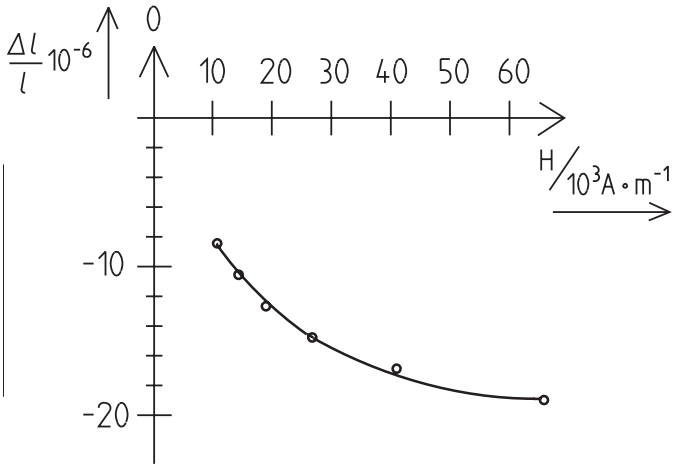

In nickel the rod became shorter (sink of circular interference fringes); therefore, a negative magnetostriction existed in this case (see Fig. 7 and Table 2).

Table 2

I/A	H/A/m (see (9))	Ring-changes/n	Δl/m (see (10))	$\Delta l/l$ with l =0.15 m
0.53	10600	4	$-1.27 \cdot 10^{-6}$	$-8.44 \cdot 10^{-6}$
0.71	14200	5	$-1.58 \cdot 10^{-6}$	$-10.55 \cdot 10^{-6}$
0.94	18800	6	$-1.90 \cdot 10^{-6}$	$-12.67 \cdot 10^{-6}$
1.33	26600	7	$-2.21 \cdot 10^{-6}$	$-14.77 \cdot 10^{-6}$
2.04	40800	8	$-2.53 \cdot 10^{-6}$	$-16.87 \cdot 10^{-6}$
3.28	65600	9	$-2.84 \cdot 10^{-6}$	$-18.98 \cdot 10^{-6}$

The comparison with the literature values (Fig. 4) exhibited good agreement. In copper no alteration in length can be detected for a rapid current elevation. It may be possible that a slow heating of the material would show changes in the circular interference rings over a long period of time.

Diffraction intensity of multiple slits and grids

LEP 2.3.04 -00

Related topics

Huyghens principle, interference, Fraunhofer- und Fresnel-diffraction, coherence, laser.

Principle

Multiple slits which all have the same width and the same distance among each other, as well as transmission grids with different grid constants, are submitted to laser light. The corresponding diffraction patterns are measured according to their position and intensity, by means of a photo diode which can be shifted.

Equipment

Laser, He-Ne 1.0 mW, 220 V AC	08181.93	1
Universal measuring amplifier	13626.93	1
Optical profile bench l = 150 cm	08281.00	1
Base f. opt. profile-bench, adjust.	08284.00	2
Slide mount f. opt. pr.-bench, h = 30 mm	08286.01	5
Slide device, horizontal	08713.00	1
Lens holder	08012.00	2
Object holder, 5×5 cm	08041.00	1
Lens, mounted, f = +20 mm	08018.01	1
Lens, mounted, f = +100 mm	08021.01	1
Photoelement f. opt. base plt.	08734.00	1
Diaphragm, 3 single slits	08522.00	1
Diaphragm, 4 multiple slits	08526.00	1
Diffraction grating, 4 lines/mm	08532.00	1
Diffraction grating, 8 lines/mm	08534.00	1
Diffraction grating, 10 lines/mm	08540.00	1
Diffraction grating, 50 lines/mm	08543.00	1
Digital multimeter	07122.00	1
Connecting cord, l = 750 mm, red	07362.01	1
Connecting cord, l = 750 mm, blue	07362.04	1

Tasks

1. The position of the first intensity minimum due to a single slit is determined, and the value is used to calculate the width of the slit.
2. The intensity distribution of the diffraction patterns of a threefold, fourfold and even a fivefold slit, where the slits all have the same widths and the same distance among each other, is to be determined. The intensity relations of the central peaks are to be assessed.
3. For transmission grids with different lattice constants, the position of the peaks of several orders of diffraction is to be determined, and the found value used to calculate the wavelength of the laser light.

Set-up and procedure

Experimental set-up is shown in fig. 1. With the assistance of the f = 20 mm and f = 100 mm lenses, a widened and parallel laser beam is generated, which must impinge centrally on the photocell with the slit aperture, the photocell being situated approximately at the centre of its shifting range. The diffracting objects are set in the object holder. It must be made sure the diffraction objects which are to be investigated are set vertically in the object holder, and uniformly illuminated.

Caution: Never look directly into a non attenuated laser beam

Fig. 1: Experimental set-up to investigate the diffraction intensity of multiple slits and grids. (Positions of the components on the optical bench: laser = 2.5 cm; f/20 mm lens = 14.5 cm; f/100 mm lens = 27.5 mm; diffracting objects = 33 cm; slide mount lateral adjustm., calibr. = 147. 5 cm).

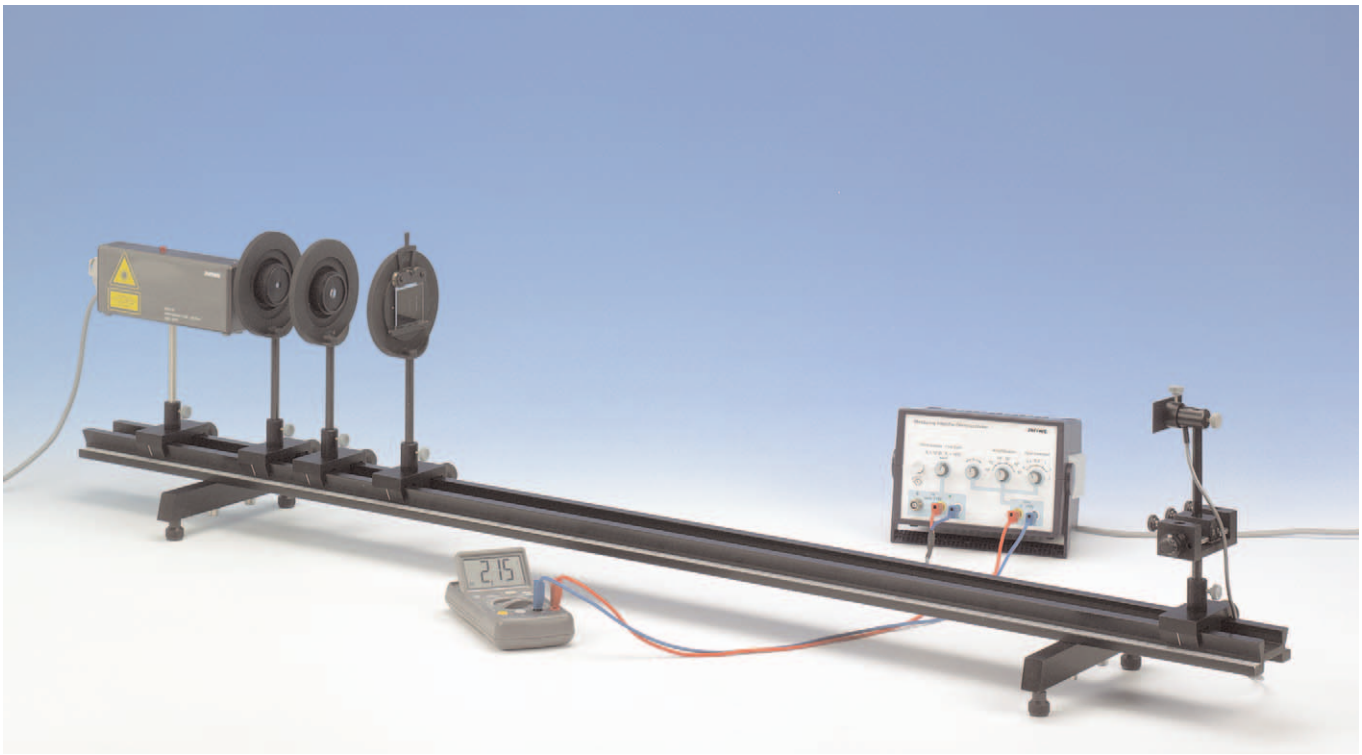

LEP 2.3.04 -00

Diffraction intensity of multiple slits and grids

The laser and the measuring amplifier should warm up for about 15 minutes before starting measurements, in order to avoid undesirable intensity fluctuations. The photocell is connected to the $10^4\Omega$ input of the measuring amplifier (amplification factor 10^3-10^5). When the amplification factor is changed, the zero point of the measurement amplifier must be checked while the photocell is covered, and corrected if necessary.
The diffraction intensity values are determined for the multiple slits by shifting the photocell in steps of 0.1 mm – 0.2 mm. For the transmission grids, the positions of diffraction peaks must be determined so as to be able to calculate the wavelength of the laser light. For the 50 lines/mm transmission grid, the secondary peaks are outside the shifting range of the photocell, so that in this case the position of the diffraction reflexes must be marked on a sheet of paper and their distance measured with a ruler.

Theory and evaluation

If monochromatic light of wavelength λ impinges on a system of parallel and equidistant slits, the following will be true for the light intensity I of beams deflected by an angle φ:

$$I(\varphi) \propto b^2 \cdot \frac{\sin^2\left(\frac{\pi}{\lambda} \cdot b \sin\varphi\right)}{\left(\frac{\pi}{\lambda} \cdot b \sin\varphi\right)^2} \cdot \frac{\sin^2\left(\frac{p\pi}{\lambda} \cdot g \sin\varphi\right)}{\sin^2\left(\frac{\pi}{\lambda} \cdot g \sin\varphi\right)} \quad (1)$$

(b = width of slit; g = distance between slits; p = number of slits)

According to Fraunhofer, the minima and the peaks of a single slit are called 1st class interferences, whereas the interaction of several slits yields 2nd class interferences.
Observing only a single slit (1st factor), this yields a minimum intensity when the numerator becomes zero. In this case, the following is valid:

$$\sin\varphi_k = \frac{k \cdot \lambda}{b} \; ; \; (k = 1, 2, 3\ldots) \quad (2)$$

The angular position of the 1st class peaks is given approximately through:

$$\sin\varphi_k{}^* = \frac{2k^* + 1}{2} \cdot \frac{\lambda}{b} \; ; \; (k^* = 1, 2, 3\ldots) \quad (3)$$

If several slits act together, the minima of the single slits always remain. Supplementary 2nd class minima appear when the 2nd factor also becomes zero.
For a double slit (p = 2), the zero points can be easily calculated by simple transformation of the 2nd factor. Equation (1) then yields:

$$4\cos^2\left(\frac{\pi}{\lambda} \cdot g \sin\varphi\right) = \pm 1 \quad (4)$$

This expression becomes zero for

$$\sin\varphi_h = \frac{2h + 1}{2} \cdot \frac{\lambda}{g} \; ; \; (h = 0, 1, 2, 3\ldots) \quad (5)$$

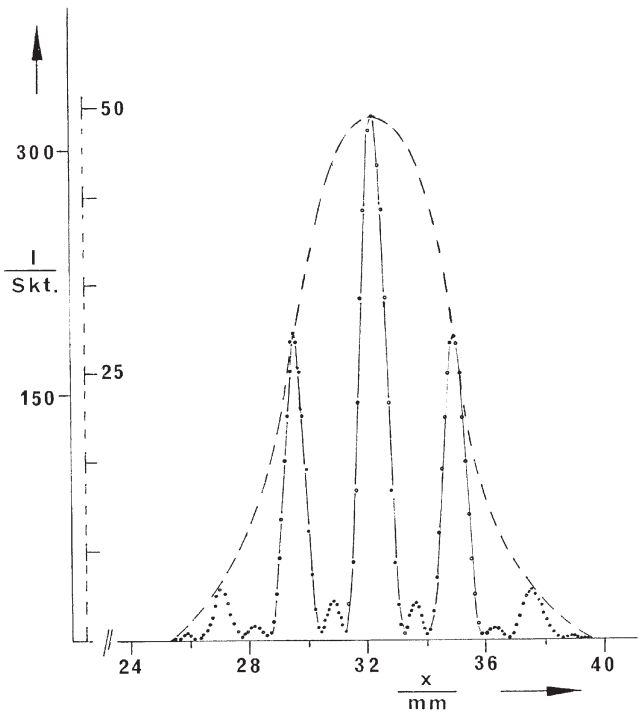

Fig. 2: Diffraction intensity I as a function of the position x for a threefold slit, b_1 = 0.1 mm and g = 0.25 mm. Distance between threefold slit and photocell: L = 107 cm. For comparison, the intensity distribution of a single slit, b = 0.1 mm, is entered as a dotted line.

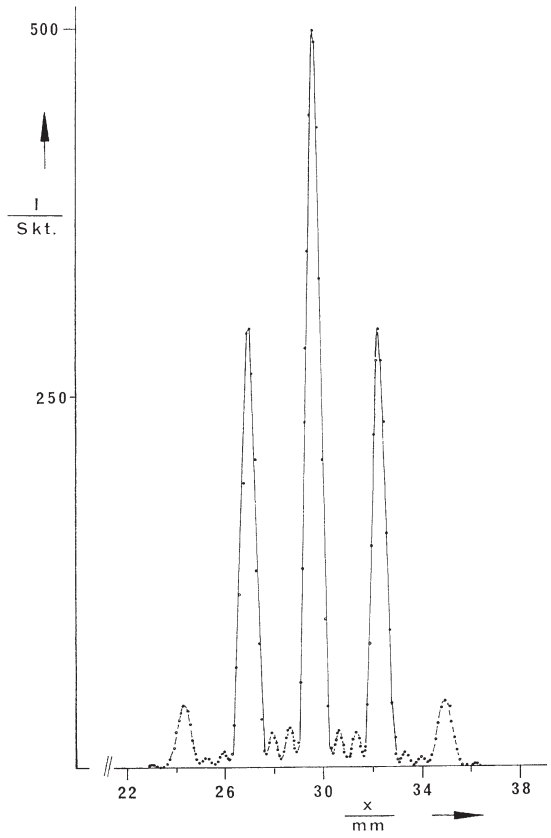

Fig. 3: Diffraction intensity I as a function of the position x for a fourfold slit with b_1 = 0.1 mm and g = 0.25 mm.

Fig. 4: Reciprocal distance of the diffraction peaks up to the 3rd order of diffraction (K = 3) as a function of the lattice constant.

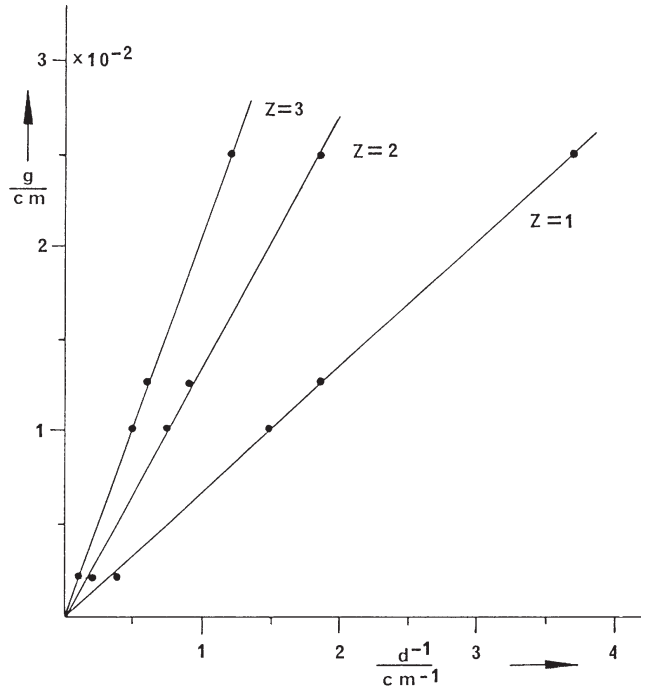

The following is valid for the intensity I of the main 2nd class peaks:

$$I \propto p^2 \qquad (6)$$

The main 2nd class peaks thus become more prominent as the number of slits increases. There still are (p - 2) secondary 2nd class peaks between the main peaks.
When light is diffracted through transmission grids with lattice constant g, the diffraction angle φ of the main peaks fulfils the following relation:

$$\sin\varphi_k = \frac{k\lambda}{g} \;;\; (k = 0,1,2,3\ldots) \qquad (7)$$

Fig. 2 shows the diffraction intensity I for a threefold slit as a function of the position x of the photocell (distance between the diffracting object and the photocell; L = 107 cm). For comparison, the diffraction pattern of a single slit is entered as an envelope, with an adapted ordinate scale.
The minima of the single slit also remain in presence of corresponding multiple slits. For these, one obtains d = 0.095 mm from (2), with the distance $2 \cdot \Delta x$ =14 mm between the two 1st class minima ($\sin\varphi \approx \tan\varphi$, L = 107 cm, λ = 632.8 nm). The number of secondary 2nd class peaks of the threefold slit is (p - 2) = 1.

Fig. 3 shows the diffraction figure of a fourfold slit. In this case, the number of 2nd class peaks is (p - 2) = 2. In the same way, diffraction through a fivefold slit (no figure) yields (p - 2) = 5-2nd class secondary peaks.
Table 1 gives the intensity values of the central peaks of the diffracting objects with p = 3 till p = 5, as well as the relative values determined empirically and according to (6).

Table 1

	exp.	theor.
I_{05} (p=5) = 720 Skt.		
I_{04} (p=4) = 500 Skt.	I_{05} / I_{04} = 1.44	$(5/4)^2$ = 1.56
I_{03} (p=3) = 300 Skt.	I_{05} / I_{03} = 2.40	$(5/3)^2$ = 2.78

Fig. 4 shows the distances between diffraction peaks measured for 4 different transmitting grids up to the 3rd order (K = 3) as a function of the lattice constant g. With (7), fig. 4 yields λ = 635 nm as an average value for the wavelength of the used laser light.

Polarisation through λ/4 plates

LP 3.2

Used concepts

Linearly, circularly and elliptically polarised light, polarizer, analyser, plane of polarisation, Malus' law, double refraction, optical axis, ordinary and extraordinary beam.

Principle

Monochromatic light impinges on a mica plate, perpendicularly to its optical axis. If the thickness of the plate is adequate (λ/4 plate), a phase shift of 90° occurs between the ordinary and the extraordinary beam when the latter leaves the crystal. The polarisation of exiting light is examined for different angles between the optical axis of the λ/4 plate and the direction of polarisation of incident light.

Equipment

Base plate with rubber feet	08700.00	1
HeNe laser	08180.93	1
Adjusting support 35 x 35 mm	08711.00	1
Surface mirror 30 x 30 mm	08711.01	1
Magnet foot	08710.00	6
Lens support	08723.00	1
Mounted lens, *f* = +20 mm	08018.01	1
Aperture support	08724.00	1
Polarisation filter	08730.00	2
Mica polarising substance	08664.00	2
Photocell, silicone	08734.00	1
Measurement amplifier, universal	13626.93	1
Voltmeter 0.3... 300 V/10 ... 300 V~	07035.00	1
Connecting cable, red, *l* = 500 mm	07361.01	2

Fig. 1: Experimental set up for polarisation through λ/4 plate (* only required for 5 mW laser)

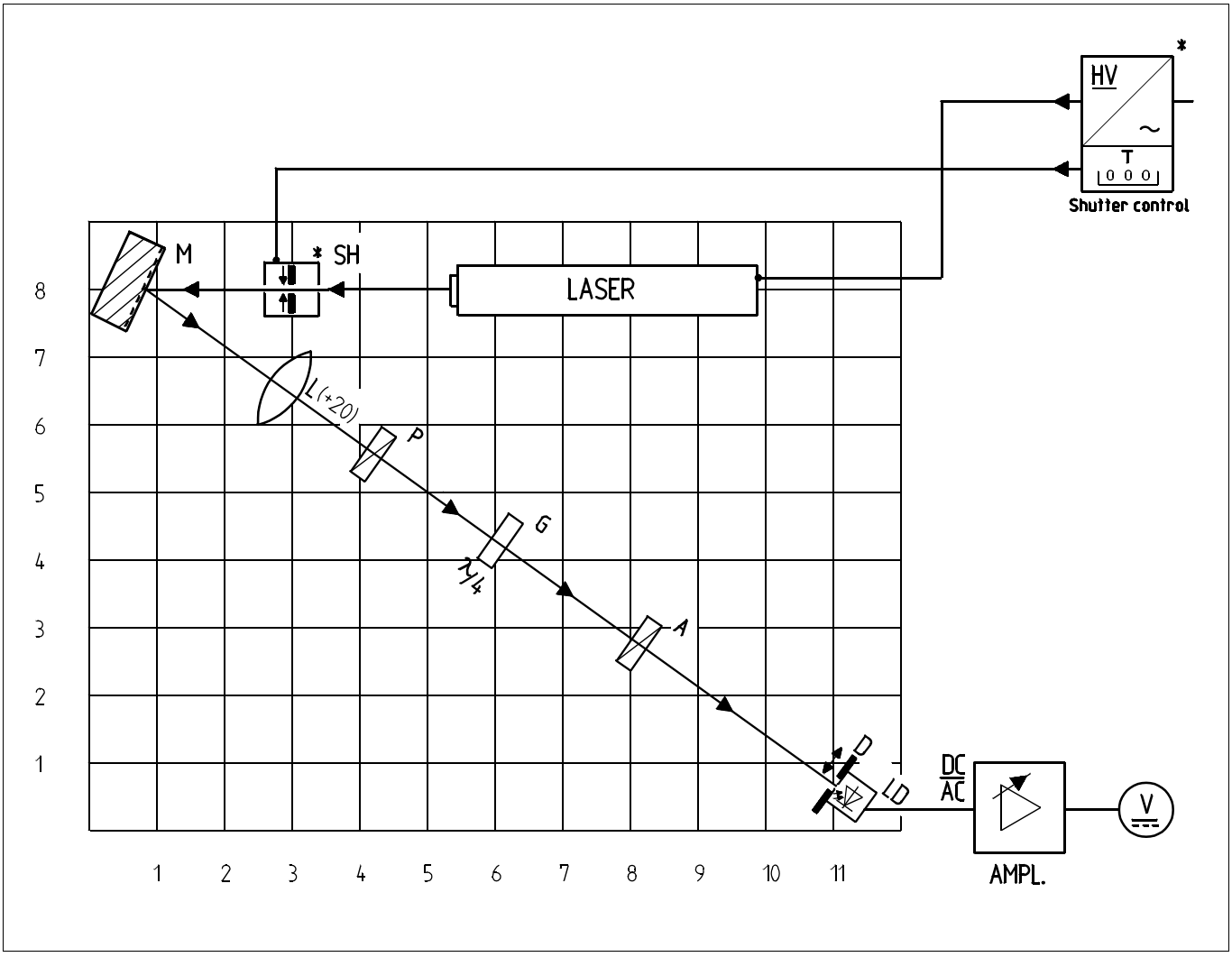

LP 3.2

Polarisation through λ/4 plates

Problem

1. Measurement of the intensity of linearly polarised light as a function of the analyser's position (Malus' law: $I = I_0 \cos^2\phi$).
2. Measurement of light intensity after the analyser as a function of the angle between the optical axis of the λ/4 plate and the analyser.
3. Carrying out experiment (2) with two successive λ/4 plates.

Set-up and performance

— The experimental set up is shown in fig. 1. The recommended set up height (height of beam path) should be 130 mm.
— To begin with, the beam path is adjusted without λ/4 plate **G** in such a way that photocell **LD** is well illuminated. (Adjust amplification in so that voltage does not increase above the allowed maximum).
— The zero of the universal measurement amplifier is adjusted with the laser switched off.
— With polarizer **P** set to zero, analyser **A** is rotated until the intensity of transmitted light displays a minimum.
— The λ/4 plate is clamped in the support and rotated until the light transmitted by the analyser again displays an intensity minimum.
— The direction of polarisation of light coming from the polarizer now forms an angle of 0^o (or 90^o) with the optical axis of the λ/4 plate.
— Light intensity is measured as a function of the position of the analyser within a range of -90^o and $+90^o$, for the angles 0^o, 30^o, 45^o, 60^o and 90^o of the λ/4 plate.
— Voltage supplied by the photocell is proportional to the intensity of incident light.

Theory and evaluation

Light velocity in the direction of light polarisation has the same value c_0 as in the direction of the optical axis of a double refracting crystal. Polarised light also propagates with velocity c_0 perpendicularly to the optical axis, if the electric vector is perpendicular to the optical axis (ordinary beam, fig. 2). If the electric field vector is parallel to the optical axis, light velocity $c \neq c_0$ (extraordinary beam).
E_0 is the amplitude of an electric field vector coming out or polarizer **P** and ϕ the angle between polarisation direction *P* and the optical axis of a double refracting crystal.

From fig. 2, one obtains the following relations for the field vectors of the ordinary and extraordinary beams:

$$E_1(t) = E_0(t) \cdot \sin\Phi \qquad (1a)$$

$$E_2(t) = E_0(t) \cdot \cos\Phi \qquad (1b)$$

At time *t*, the status of oscillation of the two beams at the surface of the crystal is described by:

$$E_1(t) = E_0 \cdot \sin\Phi \cdot \sin\omega t \qquad (2a)$$

$$E_2(t) = E_0 \cdot \cos\Phi \cdot \sin\omega t \qquad (2b)$$

For double refracting crystals (λ/4 plates) of thickness

$$d_{\lambda/4} = \frac{\lambda}{4} \cdot \frac{1}{n_o - n_{a0}} \qquad (3)$$

(n_0 is the refraction index of the ordinary beam, n_{a0} that of the extraordinary beam in the crystal)

Fig. 2: Splitting of polarised light in a double refracting crystal (**P** = polarizer, **A** = analyser)

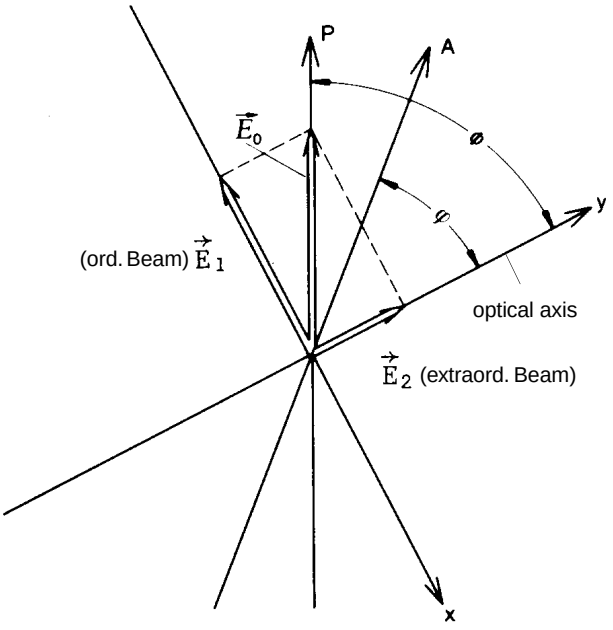

Polarisation through λ/4 plates

LP 3.2

the two beams reunite to a resulting beam when leaving the crystal. This is accompanied by a path difference of λ/4, that is, a phase difference of π/2. Equation (2) becomes:

$$E_x = E_1 = E_0 \cdot \sin\Phi \cdot \sin\omega t \quad (4a)$$

$$E_y = E_2 = E_0 \cdot \sin\Phi \cdot \sin\omega t \quad (4b)$$

(4) is the parametric representation of an *E* vector rotating around an axis in the direction of propagation. For $\phi = 0^o$ and $\phi = 90^o$, one obtains linearly polarised light with the intensity

$$J = J_0 \sim E_0^2 \quad (5)$$

For $\phi = 45^o$, one has

$$\sin\Phi = \cos\Phi = \frac{1}{\sqrt{2}}$$

and the absolute value of the rotating *E* vector is:

$$E = \sqrt{E_x^2 + E_y^2} = \frac{E_0}{\sqrt{2}} \quad (6)$$

Light is circularly polarised, with intensity

$$J = \frac{J_0}{2} \sim \frac{E_0^2}{2} \quad (7)$$

and is transmitted without being weakened for every position of analyser **A**.

For all angles $\phi \neq 0^o$, 45^o, and 90^o, transmitted light is polarised elliptically. The tip of an *E* vector rotating in the direction of propagation describes an ellipse with the half axes

$$E_a = E_0 \cdot \sin\Phi \text{ (x–direction)} \quad (8a)$$

$$E_b = E_0 \cdot \cos\Phi \text{ (y–direction)} \quad (8b)$$

For light intensities transmitted by the analyser in the corresponding directions, the following relations hold:

$$J_a \sim E_a^2 = E_0^2 \cdot \sin^2\Phi \quad (9a)$$

$$J_b \sim E_b^2 = E_0^2 \cdot \cos^2\Phi \quad (9b)$$

Fig. 3: Intensity distribution of linearly polarised light as a function of analyser position (without λ/4 plate)

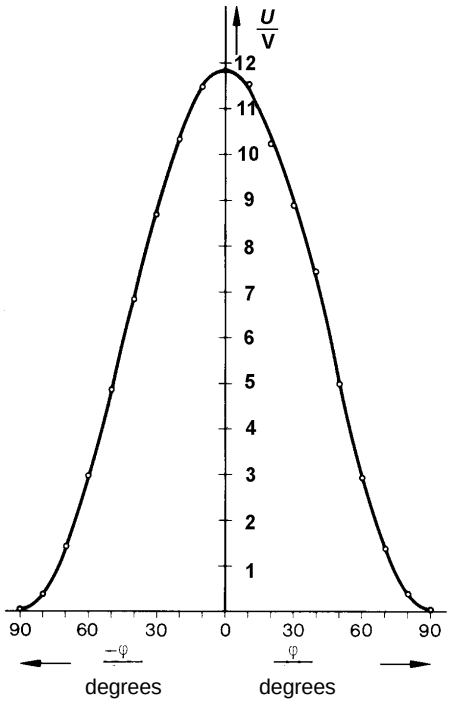

Fig. 4: Intensity distribution of polarised light for different angles of the λ/4 plate, as a function of the analyser position)

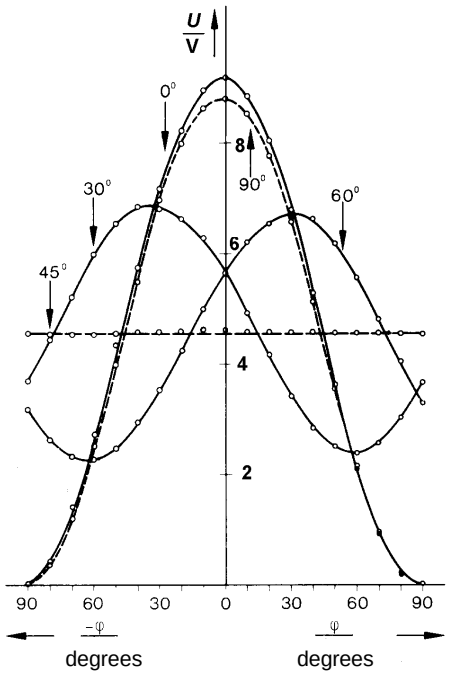

LP 3.2

Polarisation through λ/4 plates

When the analyser is rotated, one obtains for the relation between maximum and minimum transmitted light intensity:

$$\frac{J_a}{J_b} = \frac{E_a^2}{E_b^2} = \frac{\sin^2 \Phi}{\cos^2 \Phi} = \tan^2 \Phi \qquad (10)$$

For an arbitrary angular position of the analyser as compared to the optical axis of the λ/4 plates, the following is valid (Fig.2):

$$J \sim E_0^2 \cdot \cos^2\Phi \cdot \cos^2\varphi + E_0^2 \cdot \sin^2\Phi \cdot \sin^2\varphi \qquad (11)$$

To start with, the intensity distribution of linearly polarised light is measured without λ/4 plate in the beam path as a function of analyser position (fig. 3). The form of polarisation of the outgoing light is determined from the corresponding intensity distributions for different angles between the optical axis of the λ/4 plate and the transmitting direction of the analyser.
In case of two successive λ/4 plates, linearly polarise light is generated for all angles
between the optical axis of the thus formed λ/2 plate (fig. 5).

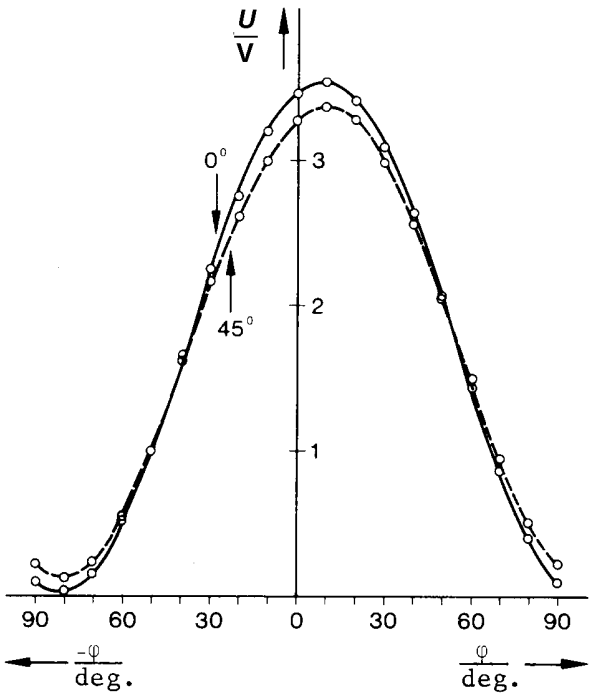

Fig. 5: Intensity distribution of polarised light for different angular positions of a λ/2 plate